



Vacuum-based Robotic Gripper using Vacuum Generator and Soft Suction Cup for Pick-and-Place of Electronic PCB Boards

Muhammad Syafiq Sheik Azmi*, Muhamad Hisyam Rosle**, Muhammad Nazrin Shah Shahrol Aman*(C.A.), Ali Akbar Abd Aziz*** and Chandran Tetegre***

Abstract: The automation of Printed Circuit Board (PCB) assembly using robotic arms is increasingly essential in the electronics manufacturing industry, driven by the need for high precision and efficiency. A significant challenge in this process is the delicate handling and accurate placement of various types of PCB boards, such as SATA M.2, mSATA, and SATA Slim. This research aims to design and evaluate a vacuum-based robotic gripper using a vacuum generator and soft suction cup for the pick-and-place operations of electronic PCB boards. The methodology involves the design, fabrication, and experimental testing of the vacuum gripper, analyzing its performance across different feed pressures and vacuum levels. The principal results show that the vacuum gripper is highly effective in securely handling different PCB types, with success rates improving significantly at higher feed pressures, particularly at 0.3 MPa where all three PCB types attained perfect success rates of 100%. Specifically, the vacuum flow rates at a vacuum level of 80 kPa were 0.0010 NL/s, 0.002 NL/s, and 0.0030 NL/s for feed pressures of 0.1 MPa, 0.2 MPa, and 0.3 MPa, respectively. These findings confirm the vacuum gripper's capability to enhance automation in PCB assembly, offering a scalable and adaptable solution that meets the industry's demands for precision, efficiency, and reliability. Overall, the vacuum gripper demonstrated a 100% success rate for all tested PCB types at optimal feed pressure, significantly improving. This study provides a foundation for future improvements in robotic handling systems for delicate electronic components.

Keywords: Vacuum-based robotic gripper; PCB assembly automation; pick-and-place operations; electronic components handling.

1 Introduction

THE automation of PCB assembly using robotic arms is becoming increasingly predominant in the electronics manufacturing industry. A pivotal process in

PCB assembly is the pick-and-place operation, where electronic components are accurately placed onto the PCB. This paper compares the handling characteristics of SATA M.2, mSATA, and SATA Slim PCBs using a 6-axis robot arm equipped with a suction-based end effector. Each PCB type has different physical and handling characteristics that impact the pick-and-place process [1]. The integration of such robotic arms into PCB assembly lines addresses challenges such as object orientation and placement accuracy, which are crucial for maintaining the high quality and reliability of electronic devices [2].

A suction gripper, also known as a vacuum gripper, is an end effector used in 6-axis robotic arms for handling and manipulating objects, particularly in delicate and precision-demanding applications like

Iranian Journal of Electrical & Electronic Engineering, 2025.

Paper first received 05 Dec 2024 and accepted 20 Feb 2025.

* The author is with the Faculty of Electrical Engineering & Technology, Universiti Malaysia Perlis, Malaysia.

E-mail: nazrinshahrol@unimap.edu.my

** The authors are with the Department of Mechanical Precision Engineering, Malaysia-Japan International Institute of Technology, Malaysia.

*** The authors are with the Department of Engineering, SMART Modular Technologies Sdn Bhd, Malaysia.

Corresponding Author: Muhammad Nazrin Shah Shahrol Aman.

electronic PCB assembly [3]. It comprises a suction cup, typically made of rubber or silicone, which provides a firm yet gentle grip, a vacuum generator to create the necessary suction force, control valves and sensors to regulate and monitor the vacuum pressure, and a mounting interface to connect the gripper to the robotic arm [4]. Suction grippers offer non-destructive handling, versatility, precision, and repeatability, making them ideal for various tasks in PCB assembly, such as picking and placing components, handling surface mount technology (SMT) parts, and moving items through inspection systems [5]. They excel in rapidly and efficiently handling objects with smooth, non-porous surfaces, although managing vacuum pressure is crucial to prevent damage or dropping [6]. When combined with the 6-axis robotic arm's flexibility and precision, suction grippers provide a powerful solution for automated handling in precision-driven industries [7].

SATA M.2, mSATA, and SATA Slim PCBs are compact, high-speed storage solutions designed for different industry applications [8]. SATA M.2, with its versatile form factor (22mm wide and 60mm long), supports both SATA and PCIe interfaces, offering high performance, especially with NVMe, and is widely used in modern laptops, ultrabooks, and desktops [9]. mSATA, about the size of a business card (50.80mm x 29.85mm), uses the SATA interface for moderate speeds up to 6Gbps, fitting into mini PCIe slots and serving older laptops, netbooks, and compact embedded systems [10]. SATA Slim, with a slim and elongated design (54mm wide and 39mm deep), also supports up to SATA III speeds and is used in thin client computers, industrial PCs, and embedded systems where space is constrained [11]. Each type addresses specific needs, from high-performance consumer electronics to specialized industrial applications [12]. These PCBs are fragile and can easily be damaged by excessive force. Overall, addressing these challenges requires precise force control and careful design and control of vacuum grippers [13].

The electronics manufacturing industry increasingly demands high precision, efficiency, and reliability in PCB assembly processes due to the growing complexity and miniaturization of electronic components [14]. Traditional manual handling methods are prone to errors and inefficiencies, making automation essential [15]. A 6-axis robotic arm equipped with a vacuum gripper is highly sought after for its ability to perform complex movements and orientations with high precision [16]. The six degrees of freedom provided by the robotic arm enable it to reach any position within its operational envelope, while the vacuum gripper offers a gentle yet secure grip on delicate components, minimizing the risk of damage [17]. This combination ensures accurate and consistent placement of components on PCBs, significantly enhancing production quality and

throughput. The core problem is to develop and deploy a 6-axis robotic arm with a vacuum gripper capable of performing the complex movements and orientations required for high-precision PCB assembly. This robotic system must be able to handle delicate electronic components without causing damage and ensure accurate placement to enhance production quality and throughput. The solution must be scalable, adaptable to various PCB designs, and cost-effective to implement across different manufacturing setups [18].

Additionally, the adoption of 6-axis robotic arms with vacuum grippers addresses the industry's need for flexibility and adaptability [19]. These robotic systems can be easily reprogrammed and reconfigured to handle different types of PCBs and components, making them suitable for a wide range of applications in consumer electronics, automotive, aerospace, and medical devices [20]. The ability to operate continuously without fatigue further increases production efficiency and reduces labor costs [21]. As the demand for more compact electronic devices continues to grow, the need for advanced automation solutions like 6-axis robotic arms with vacuum grippers will become increasingly critical to meet the industry's high standards and production goals [22].

While 6-axis robotic arms with vacuum grippers offer significant advantages in PCB assembly, they also have limitations. One major limitation is their reliance on smooth, non-porous surfaces to maintain a secure grip, which can be problematic for handling components with uneven or permeable surfaces [23]. Additionally, the vacuum gripper's suction force must be precisely controlled to avoid dropping or damaging delicate components, requiring sophisticated sensors and control systems [24]. For performing such tasks, a pressure gauge added to the system to control the pressure of the vacuum gripper is essential. Nevertheless, the design of a suitable vacuum gripper, specifically to meet the requirements of handling thin and delicate electronic PCB boards, remains challenging. This vacuum gripper must provide a secure yet gentle grip to avoid damaging the fragile components and substrates [25]. In addition, the analysis of the vacuum gripper with different suction forces on different electronic PCB boards is yet to be verified.

The main contributions of the present work include (1) the design of a vacuum gripper for manipulating electronic PCB boards, and (2) the analysis of the performance of the vacuum gripper with different suction forces on different electronic PCB boards. The methodology discusses the structure, principal, and the fabrication process of the vacuum gripper and vacuum generator, system configuration and board specification. The results present the comparison of vacuum flow between different types of PCBs. The final part presents the discussion and conclusion.

1. Methodology

1.1 Principal and Fabrication of Vacuum Gripper

The structure of the end effector of a 6-axis robotic arm using a vacuum gripper primarily consists of several key components: suction cups, vacuum channels and connecting hoses, as shown in Figure 1. The suction cups are made from conductive NBR. These cups are connected to a system of vacuum channels and hoses that link to the vacuum generator, which can be an external pump or an integrated device. The end effector is mounted on the robotic arm via a standardized interface, allowing for secure attachment and easy replacement or modification. Additionally, control valves and sensors are integrated to manage and monitor the vacuum pressure, ensuring consistent and reliable gripping performance.

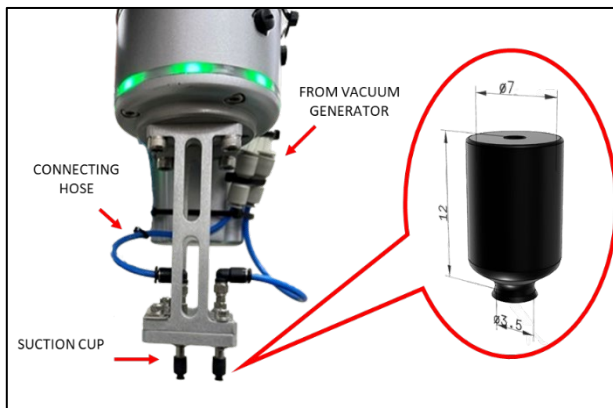


Fig. 1. Vacuum Gripper

The principle of operation for a vacuum gripper is based on creating a pressure differential. When the vacuum generator is activated, it removes air from the suction cups, creating a low-pressure area inside the cups compared to the ambient atmospheric pressure. This pressure differential generates a suction force that holds the object against the cups. The fabrication process of the end effector involves precision manufacturing of the suction cups and channels to ensure airtight seals and robust connections. The suction cups are securely attached to the vacuum channels, ensuring all connections are secure and leak-free. The proposed system of vacuum gripper functions effectively in various pick up the PCB, providing reliable and precise handling of components.

1.2 Vacuum Generator Principal

A vacuum generator uses compressed air to create a vacuum by means of the Venturi effect. When compressed air passes through a constricted section of the generator, it speeds up and creates a low-pressure area, resulting in a vacuum. Figure 2 illustrates the piINLINE® vacuum generator (MINI Pi), which utilizes

the Venturi effect to generate a vacuum with compressed air. This generator features the patented COAX® cartridge technology from the company named Piab located in Sweden, which is designed for high efficiency and low energy consumption. The figure highlights the generator's lightweight inline design, making it easy to install and handle. It also showcases various cartridge options like Si for extra vacuum flow, Pi for high performance at low feed pressures, and Xi for high flow and deep vacuum. These features enable the vacuum generator to create the necessary suction force for the robotic gripper system, ensuring effective and energy-efficient operation.



Fig. 2. piINLINE® vacuum generator (MINI Pi)

Figure 3 provides a dimensional drawing of the vacuum generator, detailing its physical structure and measurements. This drawing includes precise dimensions, crucial for integrating the vacuum generator into the overall system design. Accurate dimensions ensure that the generator fits correctly with the robotic arm and other components, maintaining a compact and efficient system layout. The detailed measurements facilitate the manufacturing and assembly process, allowing precise fabrication and alignment within the robotic gripper system. This figure underscores the importance of precision in designing automation solutions, as minor deviations in dimensions can significantly impact system performance and reliability.

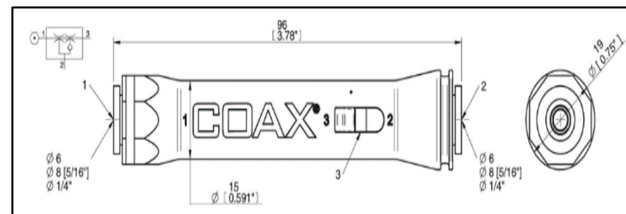


Fig. 3. Dimensional drawing of Vacuum Generator

The figures highlight the sophisticated design and engineering of the vacuum generator, which is central to the vacuum-based robotic gripper system's functionality. The combination of efficient technology, customizable options, and precise dimensions ensures that the system meets the high demands of precision, efficiency, and reliability required for PCB assembly operations.

1.3 System Configuration

The system configuration for the pick-and-place PCB operation using a 6-axis robotic arm, as depicted in the figure, involves several interconnected components working together to achieve precise and efficient handling of PCBs. Figure 4 illustrates the physical layer of the system configuration for pick-and-place operations using a 6-axis robotic arm equipped with a vacuum gripper. The central component of this system is the 6-axis robotic arm, which provides the necessary degrees of freedom for versatile movement and positioning. Attached to this robotic arm is a vacuum gripper designed to securely pick up and place PCBs using suction technology enhanced by COAX® cartridge options for optimized performance. The robotic arm and vacuum gripper are controlled by a dedicated controller unit that processes commands and coordinates the movements of the robotic system. This controller is linked to a PC running Ubuntu 18.04 with ROS (Robot Operating System) Melodic, which provides a robust platform for programming, monitoring, and adjusting the robot's tasks. The PC interface allows operators to input tasks, adjust parameters, and monitor system performance in real-time. Additionally, safety features such as emergency stop buttons are integrated into the control system to ensure safe operation.

The physical layer configuration shown in Figure 4 is designed to achieve high precision and efficiency in the automated handling of PCBs. The 6-axis robotic arm, with its flexibility and range of motion, is capable of performing complex movements and orientations necessary for accurate pick-and-place operations. The integration of a vacuum gripper, enhanced with COAX® cartridge technology, ensures a secure grip on the delicate PCBs, minimizing the risk of damage during handling. The controller unit and the PC running ROS Melodic form the backbone of the control system, enabling precise and real-time control over the robotic arm's movements. The use of ROS provides a powerful and flexible framework for robot programming and task execution, allowing for sophisticated automation and easy adaptation to different tasks and PCB types. Real-time monitoring and parameter adjustment capabilities are crucial for maintaining optimal performance and quickly addressing any issues that may arise during operation.

Safety features such as emergency stop buttons are essential in an industrial setting, ensuring that the system can be quickly halted in case of an emergency, thereby protecting both the equipment and human operators. Overall, the physical layer configuration in Figure 4 demonstrates a well-integrated and robust system designed to meet the high demands of modern PCB assembly, offering precision, efficiency, and reliability in automated pick-and-place operations. This setup not only enhances production quality and throughput but

also provides a scalable and adaptable solution for various industrial applications.

Figure 5 illustrates the system configuration for a 6-axis robotic arm used in pick-and-place operations for printed circuit boards (PCBs). This configuration includes multiple interconnected components coordinated through a central Robot Operating System (ROS) driver.

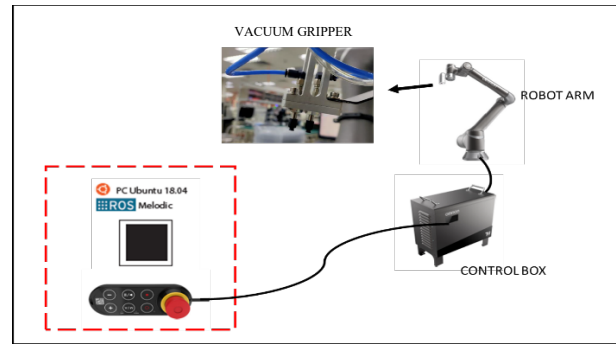


Fig. 4. Physical Layer of system

On the left side, the blue block represents the controllers and drivers, which communicate directionally to gather data and control the robot arm's movements. The ROS driver serves as a central hub, facilitating seamless communication and coordination among various system components.

On the right side, the red block represents the processor and vacuum gripper. The processor handles tasks such as object detection and position correction, while the vacuum gripper performs the actual pick-and-place operations. These components also communicate directionally to exchange necessary information. The overall workflow involves the controller gathering data and sending it to the driver, which moves the robot arm accordingly. The ROS driver coordinates with the vision processor to process visual data and command the vacuum gripper to perform the pick-and-place tasks.

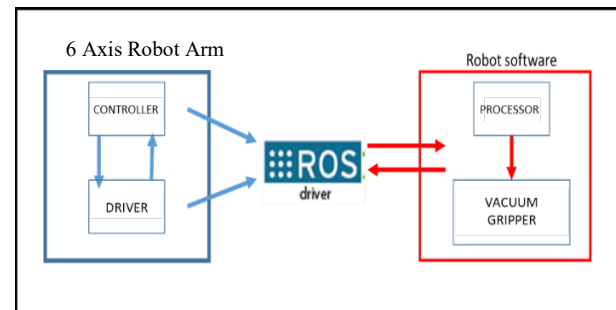


Fig. 5. Software Layer of system.

The system configuration depicted in Figure 5 is designed to ensure precise and efficient operation of the 6-axis robotic arm for PCB handling. The integration of controllers, drivers, and processors with the ROS driver enables real-time data exchange and coordination, which

is crucial for maintaining accuracy and efficiency in the pick-and-place process. The bidirectional communication between components ensures that the system can adapt to dynamic changes and perform tasks through high precision. The inclusion of a vision processor for object detection and position correction highlights the system's capability to handle complex tasks and adjust in real time, enhancing the reliability and effectiveness of the pick-and-place operations. Additionally, the use of a vacuum gripper for the actual handling of PCBs underscores the importance of maintaining a secure yet gentle grip on delicate electronic components, preventing damage while ensuring accurate placement.

This system configuration represents the advanced automation and integration required for modern electronics manufacturing. By leveraging the capabilities of ROS and sophisticated control systems, the setup ensures high precision, efficiency, and reliability, meeting the stringent demands of PCB assembly processes. This approach not only improves production quality and throughput but also provides a scalable and adaptable solution for various industrial applications.

1.4 Board Specification

Three PCB board were choose to be analyze the performance of the vacuum gripper which is SATA M.2, mSATA, and SATA Slim. Each PCB type has distinct physical and handling characteristics that impact the pick-and-place process.

2.4.1 SATA M.2

Figure 6 presents the dimensional drawing of a SATA M.2 PCB, measuring 22mm in width and 60mm in length. This PCB type is known for its compact and lightweight design, typically weighing around 6 grams. The SATA M.2 PCB is usually single-sided with connectors on one edge, necessitating precise alignment during pick-and-place operations due to its small size.

The small dimensions and lightweight nature of the SATA M.2 PCB make it suitable for high-speed and efficient handling with minimal suction force. However, the compact size demands high precision to avoid misalignment during the pick-and-place process. This highlights the importance of the vacuum gripper's precision in accurately positioning such delicate components without causing damage.

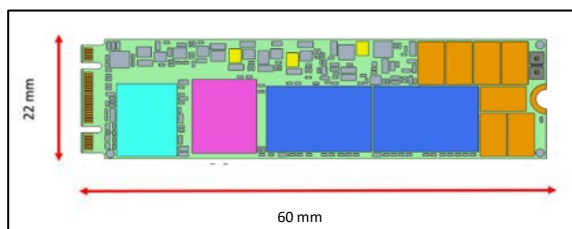


Fig. 6. Dimension drawing of SATA M.2

2.4.2 Msata

Figure 7 shows the dimensional drawing of an mSATA PCB, measuring 29.85mm in width and 50.8mm in length, and weighing around 7 grams. The mSATA PCB is slightly larger than the SATA M.2 but still relatively lightweight, requiring careful handling to avoid damage to its features and components.

The moderate size and weight of the mSATA PCB allow for a balanced approach in the pick-and-place process, requiring moderate suction force and precision. The handling process must be optimized to maintain efficiency while ensuring accurate alignment and secure gripping. The use of high-resolution vision systems and advanced motion algorithms can enhance the precision and control required for handling mSATA PCBs.

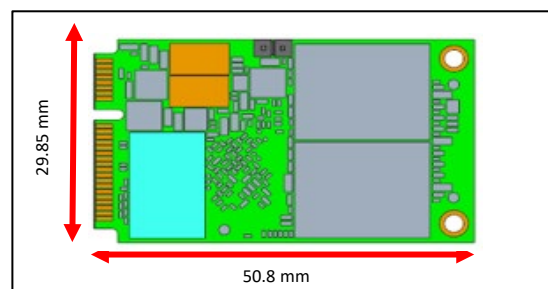


Fig. 7. Dimension drawing of mSATA

2.4.3 SATA Slim

Figure 8 provides the dimensional drawing of a SATA Slim PCB, which is 54mm in width and 39mm in length, and weighs about 15 grams. This type of PCB is larger and heavier compared to SATA M.2 and mSATA, requiring more robust handling due to its increased weight and dimensions.

The larger size and heavier weight of the SATA Slim PCB demand higher suction force and precise alignment to ensure proper seating and prevent damage. The handling process may be slower due to the need for stronger suction and higher precision, but it is crucial to balance speed and accuracy. Using adaptive suction end effectors and fine-tuning the robotic arm's movements can help manage the weight and ensure stable placement of the SATA Slim PCB.

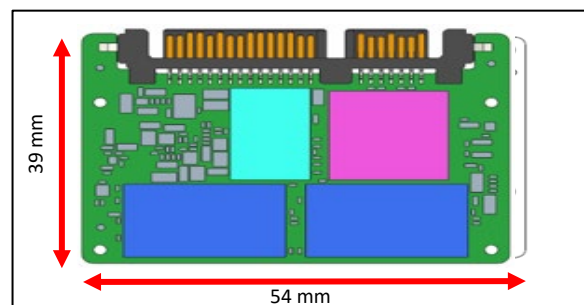


Fig. 8. Dimension drawing of SATA Slim

Overall, Figures 6, 7, and 8 highlight the varying physical characteristics and handling requirements of different PCB types. These differences emphasize the need for a versatile and adaptable vacuum gripper system capable of adjusting suction force and precision to handle a range of PCB sizes and weights effectively. The ability to handle these diverse requirements is critical for maintaining the integrity and functionality of the PCBs during automated pick-and-place operations.

1.5 Experimental setup

Figure 9 shows the workspace setup for the pick-and-place operations of PCBs using a 6-axis robotic arm equipped with a vacuum gripper. The setup includes a conveyor belt, the robotic arm with the vacuum gripper, and a PCB tray. The conveyor belt transports PCBs to the robot's workspace, where they are precisely positioned for the vacuum gripper to pick them up. The robotic arm then moves the PCBs to the designated slots in the PCB tray, which securely holds them once placed.

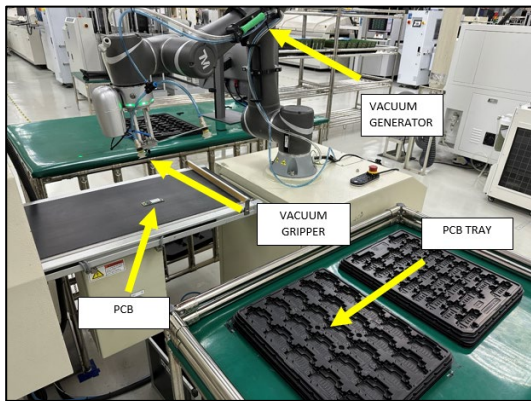


Fig. 9. Workspace setup for Pick and Place

The configuration in Figure 9 highlights the integration of various components to create an efficient and precise pick-and-place system. The conveyor belt plays a crucial role in delivering PCBs to the robot's workspace, ensuring a continuous supply of components for the pick-and-place operations. Accurate calibration of the robot's movement coordinates is essential to ensure the robotic arm can consistently and reliably grasp each PCB from the conveyor.

The PCB tray is strategically placed in line to the robot, featuring multiple slots to securely hold the PCBs once placed. This setup allows for efficient handling and organization of the PCBs, minimizing the risk of damage during transportation and placement. The vacuum gripper, connected to a vacuum generator, provides the necessary suction power to securely hold and transport the PCBs without causing damage. The workspace setup includes a user interface with control buttons for starting, stopping, and adjusting the robot's operations. This interface allows operators to manage the system effectively, ensuring smooth and uninterrupted pick-and-

place operations. Additionally, the setup's design emphasizes the importance of maintaining a clean and organized workspace to prevent any interference or errors during the pick-and-place process.

Overall, Figure 9 illustrates a well-coordinated and streamlined setup for automated PCB handling, combining precision, efficiency, and reliability. The integration of the conveyor belt, robotic arm, vacuum gripper, and PCB tray creates a cohesive system capable of meeting the high demands of modern electronics manufacturing. This setup not only enhances production quality and throughput but also provides a scalable solution adaptable to various industrial applications.

2. Result

2.1 Pick and Place Test Procedure

The process of picking and placing SATA M.2, mSATA and SATA Slim module using a vacuum gripper is shown in Fig. 10(a), 10(b), and 10(c). Initially, the vacuum gripper securely firmly grasps the SATA M.2 module from its initial position, ensuring a firm grip to prevent damage or misalignment. The gripper then moves along the z-axis, which is a vertical motion, to position the module correctly above the tray. Finally, the gripper carefully places the SATA M.2, mSATA and SATA Slim module into its designated slot in the tray. This process is automated and ensures precise and efficient handling of the module, which is essential for maintaining the integrity and functionality of the components during manufacturing or assembly.

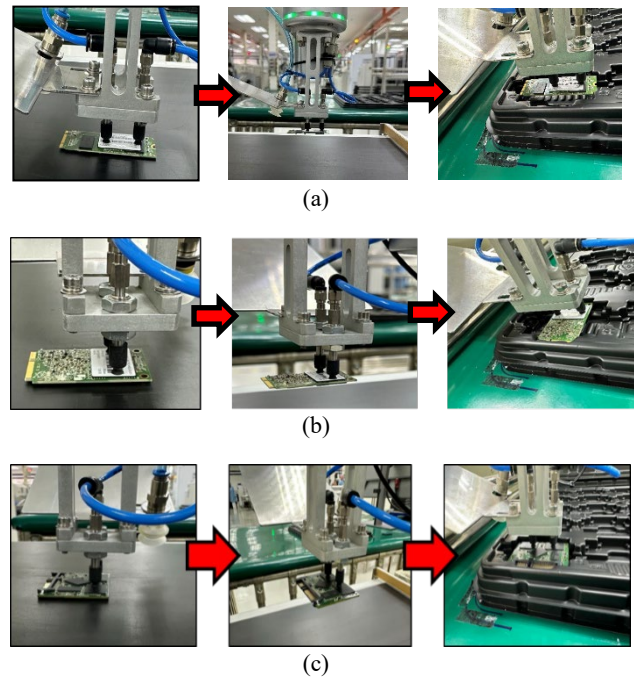


Fig. 10. Process of picking and placing (a) SATA M.2 module, (b) mSATA module, and (c) SATA Slim module.

The image illustrates in Fig. 11(a), 11(b) and 11(c) shows a SATA M.2 module, an mSATA module, and a SATA Slim module being accurately positioned within their respective slots in the tray. The precise placement ensures secure and stable fitting, essential for subsequent manufacturing or assembly steps. Each module type has been placed correctly, aligning with the defined positions in the tray, which helps streamline the workflow and maintain the integrity of the components during handling and transportation. The attention to detail in positioning highlights the importance of precision in the process to prevent damage and ensure optimal functionality of the modules.

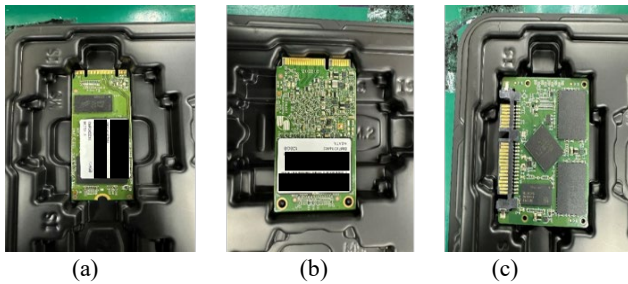


Fig. 11. Final position of each board placed on a tray for (a) SATA M.2, (b) mSATA, and (c) SATA Slim.

2.1.1 Trial of Pick and Place Test

The graph visualizes the success rates of the pick and place process for SATA M.2, mSATA, and SATA Slim PCBs across various feed pressures ranging from 0.1 MPa to 0.3 MPa. It highlights that at lower feed pressures (0.1, 0.15, and 0.2 MPa), none of the PCBs achieve any success, with all rates at 0/8. However, as the feed pressure increases to 0.25 MPa, there is a marked improvement: SATA M.2 and mSATA achieve success rates of 8/8 and 6/8, respectively, while SATA Slim achieves a success rate of 3/8. At the highest pressure tested (0.3 MPa), all three PCB types attain perfect success rates of 8/8.

SATA M.2 requires only a feed pressure of 0.2 MPa to achieve a full success rate due to its lightweight and compact design, optimized material properties, and efficient attachment mechanisms. Unlike heavier and bulkier PCB like SATA Slim, the smaller size and reduced weight of the SATA M.2 mean that less force is needed to secure it during picking it up. This combination of factors allows the SATA M.2 to be securely handled and positioned with lower feed pressure, ensuring reliable performance without the need for higher pressures required by other types of boards. SATA Slim require greater force to be securely lifted and positioned during the manufacturing process. The increased pressure ensures that the suction cups used can generate sufficient holding force to handle these larger, heavier boards without slippage or misalignment. Additionally, the larger surface area of SATA Slim

demands higher pressure to maintain a stable and uniform grip, preventing damage and ensuring precision in placement. The higher feed pressure also providing a more consistent and reliable handling process. Thus, utilizing higher feed pressures is crucial for maintaining efficiency and accuracy when dealing with bulkier and more complex PCB. This indicates that higher feed pressures, specifically 0.25 MPa and 0.3 MPa, are essential for optimizing the pick and place process for these PCB types.

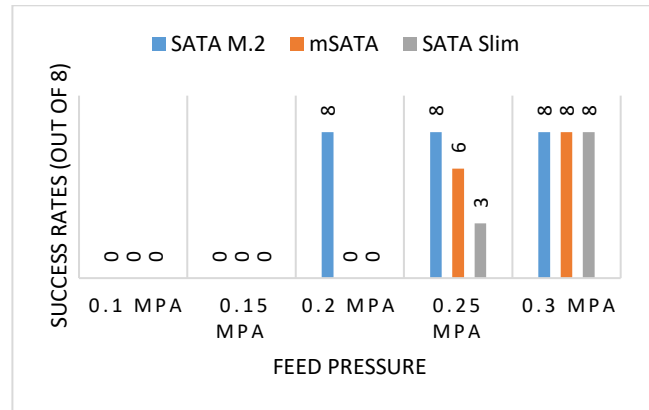


Fig. 12. Success Rate using different Feed Pressure for SATA M.2, mSATA and SATA Slim.

2.2 Vacuum Flow Validation

Table 1 provided presents the vacuum flow rates for different feed pressures of 0.1 MPa, 0.2 MPa, and 0.3 MPa, across various vacuum levels ranging from 0 kPa to 80 kPa. The vacuum levels are indicated in negative kilopascals (kPa), with values increasing in absolute magnitude (from 0 kPa to 80 kPa). Each vacuum level corresponds to a set of vacuum flow rates measured in normal liters per second (NL/s) for the specified feed pressures. For instance, at a vacuum level of 80 kPa, the vacuum flow rates are 0.0010 NL/s, 0.002 NL/s, and 0.0030 NL/s for feed pressures of 0.1 MPa, 0.2 MPa, and 0.3 MPa, respectively. As the vacuum level decreases, i.e., approaching 0 kPa, the vacuum flow rates increase for all feed pressures. This is because at higher vacuum levels (i.e., more negative values), there is a greater pressure difference between the feed pressure and the vacuum pressure, which restricts the flow of air through the system. As the vacuum level decreases and approaches 0 kPa, this pressure differential reduces, allowing air to flow more freely. Therefore, the resistance to flow is reduced, and the vacuum system can draw in more air per unit of time, resulting in higher flow rates. This behavior is consistent across different feed pressures, as the basic mechanics of pressure and flow remain the same: lower vacuum levels mean less opposition to the movement of air, so facilitating higher flow rates. Understanding this relationship is crucial for

optimizing vacuum systems in this applications, where precise control of air flow is essential.

At the lowest vacuum level (0 kPa), the vacuum flow rates reach their maximum values of 0.0800 NL/s, 0.160 NL/s, and 0.240 NL/s for the respective feed pressures. This is because there is no longer a pressure differential restricting the flow of air into the vacuum system. In other words, at 0 kPa, the vacuum level is equivalent to atmospheric pressure, meaning the system is not creating any additional resistance to air flow. This absence of a pressure differential allows the air to flow at the maximum rate permitted by the feed pressure alone. For the respective feed pressures of 0.1 MPa, 0.2 MPa, and 0.3 MPa, the flow rates are at their peak because the driving force for air flow movement is just dependent on the feed pressure without any counteracting vacuum pressure. Therefore, the flow rates of 0.0800 NL/s, 0.160 NL/s, and 0.240 NL/s represent the highest possible values that the system can achieve under these conditions, demonstrating the direct correlation between feed pressure and flow rate in the absence of vacuum-induced resistance. Understanding this dynamic is crucial for designing and operating vacuum systems to ensure optimal performance and efficiency in processes that rely on precise control of air flow. Table 1 and Figure 13 illustrates how varying vacuum levels and feed pressures impact the vacuum flow rates, providing essential data for applications that require precise control of these parameters.

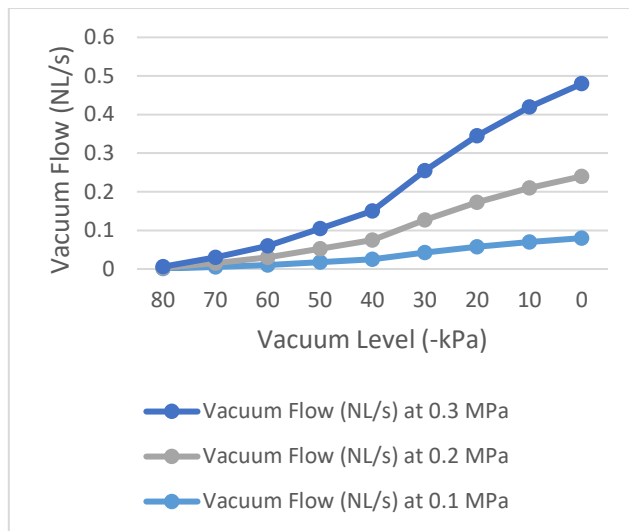


Fig. 13. Vacuum Flow for different feed pressure vs Vacuum Level

Table 1 presents the relationship between weight of each board, the required force per suction cup, the required vacuum pressure per suction cup, and the estimated vacuum flow for three different weights: 6g, 7g, and 15g. For SATA M.2 board with a weight of 6g, the required force per suction cup to successfully pick up

is 0.02943N, which corresponds to a vacuum pressure of 0.0469 kPa. We also found that the estimated vacuum flow based on trends in Table 1, of the vacuum generator to pick SATA M.2 board is 0.05 NL/s. The force per suction cup increases to 0.034335N at a vacuum pressure of 0.0547 kPa for a 7g mSATA weight. Based on Table 1, the estimated vacuum flow ranges for mSATA is from 0.05 to 0.1 NL/s. For SATA Slim weight of 15g, the force per suction cup significantly increases to 0.073575N, resulting in a vacuum pressure of 0.1171 kPa. The estimated vacuum flow from 0.1 to 0.2 NL/s for SATA Slim based on Table 1.

The result in Table 1 demonstrates that the force per suction cup and the vacuum pressure necessary to secure the object increase as the weight of the board increases. Correspondingly, the estimated vacuum flow required to maintain the suction increases with the weight, indicating a direct relationship between weight and the parameters measured. As the weight of the object increases, the force that needs to be counteracted by the suction cup also increases. This is why heavier objects require a greater force per suction cup to be held securely. Moreover, suction cups adhere to surfaces by creating a vacuum between the cup and the surface. The vacuum pressure is the difference between the atmospheric pressure and the pressure inside the cup. To hold a heavier object, the suction cup needs to create a stronger vacuum (lower pressure inside the cup) to generate a greater holding force. This results in a higher vacuum pressure reading. Furthermore, vacuum flow refers to the rate at which air must be evacuated to maintain the vacuum pressure. As the weight increases, the suction cup may need to continuously remove air to maintain the necessary vacuum pressure, especially if there are small leaks or if the surface is slightly porous. This requires a higher vacuum flow rate. In summary, heavier objects demand greater force to counteract their weight, which in turn requires higher vacuum pressure and possibly higher vacuum flow to maintain the suction. This direct relationship ensures that the suction cups can securely hold objects of varying weights.

Table 1 Analysis relationship between weight of the boards, force per suction cup, vacuum pressure per suction cup, and estimated vacuum flow for three different weights.

PCB	Weight (g)	Required Force per Suction Cup (N)	Required Vacuum Pressure per Suction Cup (kPa)	Estimated Vacuum Flow (NL/s)
SATA M.2	6	0.02943	0.0469	0.05
mSATA	7	0.034335	0.0547	0.05 - 0.1
SATA Slim	15	0.073575	0.1171	0.1-0.2

3. Conclusion

In conclusion, this study presents the design and evaluation of a vacuum-based robotic gripper equipped with a vacuum generator and soft suction cup, specifically for the pick-and-place operations of electronic PCB boards. The experimental results demonstrate the gripper's effectiveness in handling different types of PCBs, including SATA M.2, mSATA, and SATA Slim. The analysis reveals that the vacuum gripper provides reliable and precise handling of delicate PCB components by creating a strong and adjustable suction force. The success rates of the pick-and-place process significantly improve at higher feed pressures, particularly at 0.3 MPa, ensuring optimal performance for various PCB types. Additionally, the vacuum flow validation indicates a direct correlation between the vacuum levels and flow rates, essential for maintaining consistent suction force. These findings respond to the research objective by confirming the vacuum gripper's capability to enhance automation in PCB assembly, offering a scalable and adaptable solution to meet the electronics manufacturing industry's demands for high precision, efficiency, and reliability. Future work should focus on further refining the vacuum gripper design and exploring its application in handling a wider range of electronic components.

Acknowledgment

The authors would like to thank the SMART Modular Technologies Sdn. Bhd. and acknowledge the financial support provided by the Centre of Excellence for Intelligent Robotics and Autonomous Systems (CIRAS), Universiti Malaysia Perlis (UniMAP).

References

- [1] O. Rabinovich and A. Epstein, "Analytical Design of Printed Circuit Board (PCB) Metagratings for Perfect Anomalous Reflection," *IEEE Transactions on Antennas and Propagation*, vol. 66, no. 8, pp. 4086–4095, Aug. 2018, doi: <https://doi.org/10.1109/tap.2018.2836379>.
- [2] Y. Lou and S. Hua, "Research on Key Technologies of Robotic Assembly," *Applied Mechanics and Materials*, vol. 101–102, 2011, doi: <https://doi.org/10.4028/www.scientific.net/AMM.101-102.1051>.
- [3] B. Chen, J. Wan, L. Shu, P. Li, M. Mukherjee, and B. Yin, "Smart Factory of Industry 4.0: Key Technologies, Application Case, and Challenges," *IEEE Access*, vol. 6, pp. 6505–6519, Jan. 2018, doi: <https://doi.org/10.1109/access.2017.2783682>.
- [4] H. Khan, S. J. Abbasi, M. Salman, and M. C. Lee, "Super Twisting Sliding Mode Control-Based Impedance Control for Robot Arm End-Effector Force Tracking," in *Proc. 61st Annual Conf. Society of Instrument and Control Engineers (SICE)*, Sep. 2022, doi: <https://doi.org/10.23919/sice56594.2022.9905784>.
- [5] B. Micieta, P. Macek, V. Binasova, L. Dulina, M. Gaso, and J. Zuzik, "Modular Intelligent Control System in the Pre-Assembly Stage," *Electronics*, vol. 13, no. 9, p. 1609, 2024, doi: <https://doi.org/10.3390/electronics13091609>.
- [6] H. Fakhurdeen, F. Dailami, and A. Pipe, "CARA System Architecture—A Click and Assemble Robotic Assembly System," in *Proc. IEEE Int. Conf. Robotics and Automation (ICRA)*, 2019, doi: <https://doi.org/10.1109/ICRA.2019.8794114>.
- [7] D. A. Medina Portilla and V. Nandikolla, "Design of a Dexterous Robotic Arm Manipulator Using Hybrid BCI," in *ASME Int. Mechanical Engineering Congress and Exposition*, 2020, doi: <https://doi.org/10.1115/1.0004180V>.
- [8] B. Cianciotto, D. Price, L. Spencer, M. Garcia, and A. Tekes, "Design and Development of a Novel Soft Gripper Manipulated by a Robotic Arm," in *ASME Int. Mechanical Engineering Congress and Exposition*, 2021, doi: <https://doi.org/10.1115/IMECE2021-69880>.
- [9] T. J. Cairnes, C. J. Ford, E. Psomopoulou, and N. Lepora, "An Overview of Robotic Grippers," *IEEE Potentials*, 2023, doi: <https://doi.org/10.1109/MPOT.2023.3236143>.
- [10] R. Gutierrez, M. Garcia, J. McDuffie, C. Long, and A. Tekes, "Development of Wire Actuated Monolithic Soft Gripper Positioned by Robot Manipulator," in *ASME Dynamic Systems and Control Conf.*, 2020, doi: <https://doi.org/10.1115/DSCC2020-3198>.
- [11] W. Afzal, S. Iqbal, Z. Tahira, and M. Qureshi, "Gesture Control Robotic Arm Using Flex Sensor," *Automation, Control and Intelligent Systems*, vol. 6, no. 4, 2017, doi: <https://doi.org/10.11648/j.acm.20170604.12>.
- [12] B. Varghese and B. Thilagavathi, "Design and Wireless Control of Anthropomorphic Robotic Arm," in *Proc. IEEE Int. Conf. Innovations in Information, Embedded and Communication Systems (ICIIECS)*, 2015, doi: <https://doi.org/10.1109/ICIIECS.2015.7192975>.
- [13] K. Sekarsari, D. Ikhsan, and Marfin, "Design of 2 DOF Arm Robot Control System Using Ultrasonic Sensor," *IOP Conf. Ser.: Materials Science and Engineering*, vol. 550, 2019, doi: <https://doi.org/10.1088/1757-899X/550/1/012014>.
- [14] Y. Yamamoto, S. Wakimoto, T. Kanda, and D. Yamaguchi, "A Soft Robot Arm with Flexible Sensors for Master–Slave Operation," in *Proc. 8th Int. Electronic Conf. Sensors and Applications (ECSA)*, 2021, doi: <https://doi.org/10.3390/ecca-8-11311>.

- [15] H. Götz, A. Santarossa, A. Sack, T. Pöschel, and P. Müller, "Soft Particles Reinforce Robotic Grippers: Robotic Grippers Based on Granular Jamming of Soft Particles," *Granular Matter*, 2021, doi: <https://doi.org/10.1007/s10035-021-01193-4>.
- [16] C. Davenport, F. Parietti, and H. Asada, "Design and Biomechanical Analysis of Supernumerary Robotic Limbs," in *ASME Dynamic Systems and Control Conf.*, 2012, doi: <https://doi.org/10.1115/DSCC2012-MOVIC2012-8790>.
- [17] Yu and F. Chen, "Inverse Kinematic Solution of 6-DOF Robot-Arm Based on Dual Quaternions and Axis Invariant Methods," *Arabian J. for Science and Engineering*, vol. 47, no. 12, pp. 15915–15930, 2022, doi: <https://doi.org/10.1007/s13369-022-06794-6>.
- [18] S. Leder, H. Kim, M. Sitti, and A. Menges, "Enhanced Co-design and Evaluation of a Collective Robotic Construction System for the Assembly of Large-scale In-plane Timber Structures," *Automation in Construction*, vol. 162, p. 105390, June 2024, doi: <https://doi.org/10.1016/j.autcon.2024.105390>.
- [19] V. M. S. Reddy, Y. N. K. Reddy, R. Manideep, K. S. Kumar, U. Srivastav, and M. Kalpana, "Design and Fabrication of 3D-Printed Robotic Arm by Using Stepper Motor," *Int. J. Research in Applied Science and Engineering Technology*, vol. 12, no. 4, pp. 1556–1565, 2024, doi: <https://doi.org/10.22214/ijraset.2024.60124>.
- [20] Y. Wen, C. Chen, Z. Lyu, Y. Liang, and Z. Zhang, "Design and Application of Bidirectional Soft Actuator With Multiangle Chambers," *Industrial Robot*, July 2024, doi: <https://doi.org/10.1108/ir-04-2024-0136>.
- [21] B. Xie, M. Jin, J. Duan, Z. Li, W. Wang, M. Qu, and Z. Yang, "Design of Adaptive Grippers for Fruit-Picking Robots Considering Contact Behavior," *Agriculture*, vol. 14, no. 7, p. 1082, 2024, doi: <https://doi.org/10.3390/agriculture14071082>.
- [22] D. Diachenko, A. Partyshev, S. Pizzagalli, Y. Bondarenko, T. Otto, and V. Kuts, "Industrial Collaborative Robot Digital Twin Integration and Control Using Robot Operating System," *J. Machine Engineering*, Apr. 2022, doi: <https://doi.org/10.36897/jme/148110>.
- [23] B. S. Seibel, "Vacuum Pumps: Direct Control of Vacuum and Grip," in *CRC Press eBooks*, pp. 64–65, 2024, doi: <https://doi.org/10.1201/9781003525639-24>.
- [24] J. Luo, X. Zhou, C. Zeng, Y. Jiang, W. Qi, K. Xiang, M. Pang, and B. Tang, "Robotics Perception and Control: Key Technologies and Applications," *Micromachines*, vol. 15, no. 4, p. 531, 2024, doi: <https://doi.org/10.3390/mi15040531>.
- [25] C.-N. Wang, N.-L. Nhieu, and T.-A. Pham Viet, "Enhancing Efficiency in PCB Assembly for the Leading Global Electronics Manufacturing Services Firm: A TRIZ and Ant Colony Optimization Approach," *Int. J. Advanced Manufacturing*

Technology, July 2024, doi: <https://doi.org/10.1007/s00170-024-14025-5>.

Biographies



Muhammad Syafiq Bin Sheik Azmi was born in Penang, Malaysia in 2000. He received his Bachelor of Engineering degrees in Electrical Engineering Technology (Robotics and Automation Technology) from Universiti Malaysia Perlis (UniMAP), Perlis, Malaysia, in 2023. He is currently pursuing the M.Sc. degree in Mechatronic Engineering with the Universiti Malaysia Perlis (UniMAP), Perlis, Malaysia. His current research interests include 6-axis robot arm automation, Printed Circuit Board (PCB) assembly, suction cup and normal gripper end effector.



Dr. Muhammad Hisyam Rosle was born in Malaysia in 1988. He received his Bachelor of Engineering and Master of Engineering degrees in Mechanical and Robotics Engineering from Ritsumeikan University, Shiga Prefecture, Japan, in 2011 and 2013, respectively. In 2013, he joined Toyota Auto Body (Malaysia) as a Production Engineer. From 2020 to 2021, he served as a Senior Researcher at Ritsumeikan University, focusing on the development of soft tactile sensors for robotic arms in automated pick-and-place tasks. Between 2021 and 2024, he was a Senior Lecturer in the Mechatronic Department, Faculty of Electrical Engineering and Technology, Universiti Malaysia Perlis (UniMAP), Malaysia. Since September 2024, he has been a Senior Lecturer at the Malaysia-Japan International Institute of Technology (MJIIT), Universiti Teknologi Malaysia (UTM), Kuala Lumpur, Malaysia. His research interests include soft tactile sensors, soft actuators, soft robotics, and artificial intelligence.

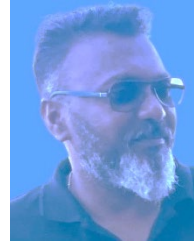


Muhammad Nazrin Shah was born in Perak, Malaysia in 1989. He received his B Eng. Degree in Mechatronic Engineering in 2013 and PhD in Mechatronic Engineering in 2019 from Universiti Malaysia Perlis (UniMAP), Malaysia. He began his career as a Research Assistant from 2013 to 2014 and continue to work as a University Fellow from 2014 to 2019 in Universiti Malaysia Perlis, (UniMAP). Currently, he is a Senior Lecturer in Faculty of Electrical Engineering Technology, Universiti Malaysia Perlis (UniMAP), Malaysia since 2019. He also a research group leader for Robotic and Automation in Medical and Sports Research Group in UniMAP Sport Engineering Research Centre and associate research fellow for Centre of Excellence for Intelligent Robotics & Autonomous Systems. His research interests include robotics, industrial automation and robotics and biomechanics.



Ali Akbar Abd Aziz was born in Penang, Malaysia in 1977. He received his Higher Diploma in Electrical and Electronic Engineering from MIDAS and Master in Industrial Engineering Technology in 2020 from Universiti Malaysia Pahang (UMP), Malaysia. He began his career as a Product Engineer from 2000 to 2006 in Celestica. He

serve as Senior Process Engineer from 2007 to 2010 in SMART Modular Technologies and promoted as Section Manager for NPI and R&D Engineering from 2010 to 2013. He continue to work as an Engineering Manager II from 2013 to 2017 and as Senior Engineering Manager from 2017 to 2024 in SMART Modular Technologies. Currently, he is a Director of SMART Modular Technologies since 2024.



Chandran Tetegre serves as Staff Engineer at SMART Modular Technologies.